



26 May 2010, 4:45 pm - 6:45 pm

## Passive Earth Pressure Force-Displacement Relationships

Patrick Wilson

*University of California at San Diego, La Jolla, CA*

Ahmed Elgamal

*University of California at San Diego, La Jolla, CA*

Follow this and additional works at: <https://scholarsmine.mst.edu/icrageesd>



Part of the [Geotechnical Engineering Commons](#)

---

### Recommended Citation

Wilson, Patrick and Elgamal, Ahmed, "Passive Earth Pressure Force-Displacement Relationships" (2010). *International Conferences on Recent Advances in Geotechnical Earthquake Engineering and Soil Dynamics*. 20.

<https://scholarsmine.mst.edu/icrageesd/05icrageesd/session01b/20>

This Article - Conference proceedings is brought to you for free and open access by Scholars' Mine. It has been accepted for inclusion in International Conferences on Recent Advances in Geotechnical Earthquake Engineering and Soil Dynamics by an authorized administrator of Scholars' Mine. This work is protected by U. S. Copyright Law. Unauthorized use including reproduction for redistribution requires the permission of the copyright holder. For more information, please contact [scholarsmine@mst.edu](mailto:scholarsmine@mst.edu).



## PASSIVE EARTH PRESSURE FORCE-DISPLACEMENT RELATIONSHIPS

**Patrick Wilson**

University of California, San Diego  
La Jolla, CA-USA 92093-0085

**Ahmed Elgamal**

University of California, San Diego  
La Jolla, CA-USA 92093-0085

### ABSTRACT

During a strong earthquake, passive earth pressure can provide resistance to excessive displacements along bridge abutments and pile caps. To account for this contribution, the force-displacement relationship is required, in addition to the peak resistance value. Experiments were performed at the University of California, San Diego to record the passive earth pressure force-displacement relationship behind a 1.7 meter tall vertical wall section. The experimental configuration of the soil container and wall system is described first. Backfill consisting of dense well-graded silty sand was placed in the soil container which measured 5.6 meters long, 2.9 meters wide and 2.15 meters deep. A finite element (FE) model is calibrated next, on the basis of this experimental response. FE analysis is then employed to compute the backfill resistance considering a range of representative backfill soils and depths. Results from these simulations help to illustrate the significant dependence on soil type and supported backfill depth on the passive force-displacement response. Calibrated hyperbolic model parameters are provided to represent the simulated passive resistance for use in practical applications.

### INTRODUCTION

Passive earth pressure provides a mechanism to resist lateral foundation movement, resulting in either an increase or a decrease in the demand placed on the other structural components. For instance, acting on the cap of a pile group (Fig. 1), passive pressure contributes to lateral stiffness and capacity (Gadre and Dobry 1998, Cole and Rollins 2006, Rollins and Cole 2006). Integral abutment bridges may mobilize passive pressure (Fig. 2) due to thermal expansion, applying a compressive load to the bridge deck (Duncan and Mokwa 2001, Peric et al. 2007, Shah 2007).

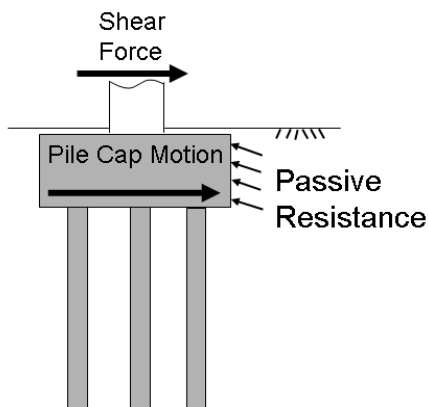


Fig. 1. Passive earth pressure acting on a pile cap

In seismic design (Caltrans 2004, Shamsabadi et al. 2007), a seat abutment system relies on the soil backfill to provide resistance to excessive longitudinal bridge deck displacement (Fig. 3). During strong shaking, if the deck impacts the abutment, a sacrificial portion (the backwall) is designed to break off into the backfill (Fig. 3). Resistance to further displacement of the deck and backwall is then provided by passive earth pressure (Shamsabadi et al. 2007).

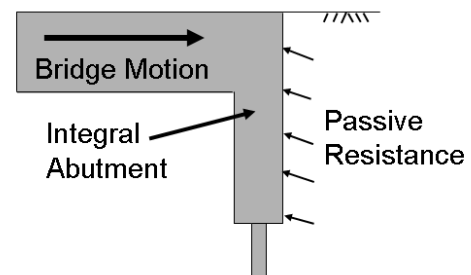


Fig. 2. Passive earth pressure acting on an integral abutment

While the Log-Spiral method (Terzaghi et al. 1996) has been shown to provide good estimates of experimentally measured peak passive resistance (Duncan and Mokwa 2001, Rollins and Cole 2006, Bozorgzadeh 2007, Lemnitzer et al. 2009), it does not offer information concerning the force-displacement relationship. For such force-displacement response, soil stiffness may substantially depend on depth (Terzaghi et al. 1996). Different types of soils used in backfills have also

shown an extensive range of variation in shear stiffness and strength (Earth Mechanics 2005).

Recently, a few large scale passive pressure load-displacement tests have been performed (Duncan and Mokwa 2001, Rollins and Cole 2006, Bozorgzadeh 2007, Lemnitzer et al. 2009). However these experiments cover only a limited range of backfill soil types and wall heights (up to 2.3 meters).

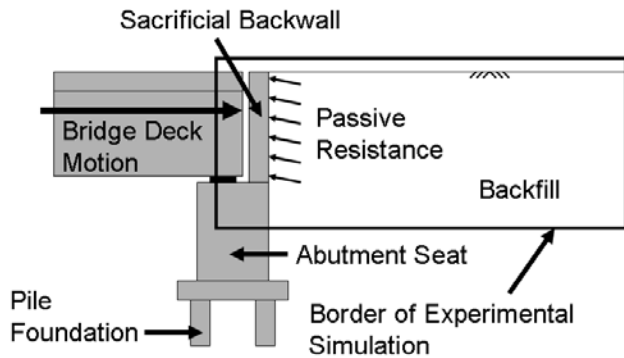


Fig. 3. Passive earth pressure acting on the sacrificial backwall portion of a seat abutment

With regard to the above issues, two additional passive earth pressure load-displacement experiments are presented first. Next, finite element (FE) models are calibrated to reproduce the observed force-displacement curves. Upon achieving a good match with the test data, the FE models are employed to produce curves for a range of backfill types and wall heights. Hyperbolic model representations of the simulated load-displacement curves are provided. These models may be useful to represent the backfill passive resistance in practical applications such as the pile cap, integral abutment, and sacrificial backwall scenarios described above (Figs. 1 through 3).

## LARGE SCALE TESTS

### Test Setup

Primary components of the experimental configuration include a large soil container (Fig. 4), a model wall section suspended from a supporting beam (Fig. 5), a loading mechanism (Fig. 6) and a compacted sandy backfill (Figs. 7 and 8). The inside dimensions of the soil container were about 2.9, 6.7 and 2.5 meters in width, length and height, respectively.

The model wall supported 1.7 meters of backfill in height, across the full container width. Additional backfill below the wall (about 0.5 meters in height) was supported by a wooden box. The walls of the container were lined on the inside with smooth plastic to minimize side friction (friction angle of 11.5 to 14 degrees, Fang et al. 2004). In that configuration, the test wall resembled a plane-strain section along the width of a seat abutment sacrificial backwall (Fig. 3).



Fig. 4. Soil container and reaction tower



Fig. 5. Test wall section and supporting beam



Fig. 6. View looking down at extended plunger jacks reacting against load cells behind test wall

Hydraulic jacks reacted through load cells onto concrete-filled steel posts (Fig. 6) to push the wall into the backfill while

measuring the applied load. Transducers also recorded the wall displacement.

Well-graded sand with about 7 percent silt content and up to 7 percent fine gravel was compacted (Fig. 8) for each test in compliance with Caltrans (2006) standard specifications for structure backfill. Soil total unit weight was approximately 20.6 kN per cubic meter. Dimensions of the backfill were about 2.9, 5.6 and 2.15 meters in width, length and height, respectively.

Direct shear and triaxial tests were performed on samples remolded as closely as possible to the experimental backfill placement conditions. From the direct shear tests, the peak friction angle  $\phi = 48$  degrees, and cohesion intercept  $c = 14$  kPa. Compared with direct shear, the triaxial tests resulted in a lower peak  $\phi = 44$  degrees, and the same  $c = 14$  kPa.



Fig. 7. Backfill placement



Fig. 8. Backfill compaction

### Test Procedure

The hydraulic jacks (Fig. 6) were used to push the test wall into the backfill during two separate tests. At the time of Test

1, the backfill was drier than the placement condition due to 23 days between construction and testing. Test 2 occurred only 3 days after the backfill was placed. In each test, the force-displacement relationship was recorded up to and beyond the peak measured resistance. In the employed testing configuration, the wall was free to move upwards with the adjacent backfill soil (similar to a relatively light anchor wall), resulting in a low mobilized wall-soil friction angle  $\delta$ .

### Test Results

In the conducted tests, the measured horizontal force increased with lateral wall displacement up to a peak value (Fig. 9), and decreased thereafter. Lacking an externally applied vertical load, the wall moved slightly upward with the adjacent backfill as it was being displaced horizontally. Consequently, the mobilized wall-soil friction  $\delta_{mob}$  was about 2 to 3 degrees based on vertical equilibrium of the model wall (Duncan and Mokwa 2001).

In terms of maximum passive resistance for these low  $\delta_{mob}$  tests (Fig. 9), the Coulomb and Log-Spiral predictions (Terzaghi et al. 1996) are essentially equal. Using  $\phi$  and  $c$  from the direct shear and triaxial tests, the Coulomb and Log-Spiral predictions were close to the measured peak passive resistance from Test 2 (with backfill conditions closest to the laboratory tested soil samples), but fell considerably short for the drier backfill of Test 1 (Wilson 2009).

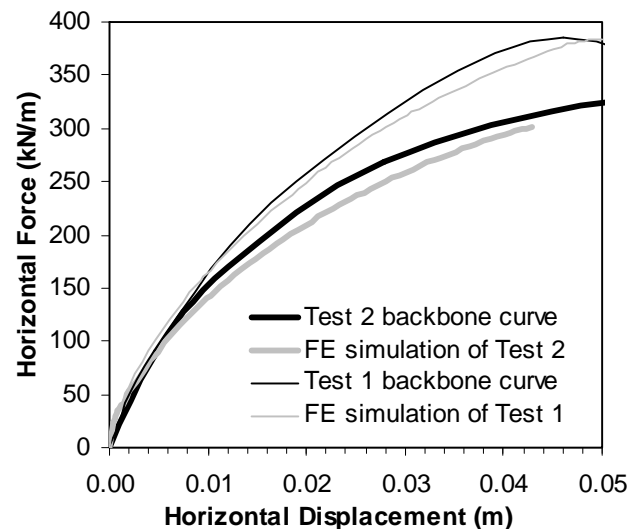


Fig. 9. Backbone force-displacement relationships from Test 1 and Test 2 compared with the FE model predictions

### FE SIMULATION OF THE EXPERIMENTS

In this section, the experimental results of Fig. 9 are compared with FE plane-strain simulations using Plaxis (2004).

## Configuration of FE Model and Boundary Conditions

For simulation of the passive pressure load-displacement experiments, the FE model backfill was 5.6 meters long and 2.15 meters tall with 1.7 meters of backfill in contact with the model wall (Fig. 10). The far end of the backfill, and the soil domain beneath the model wall were fixed in the horizontal direction and free in the vertical. To simulate the interface between the backfill and the base of the steel soil container, interface friction ( $\delta$ ) along the bottom of the model backfill was  $0.2\phi$  (McCarthy 2007).

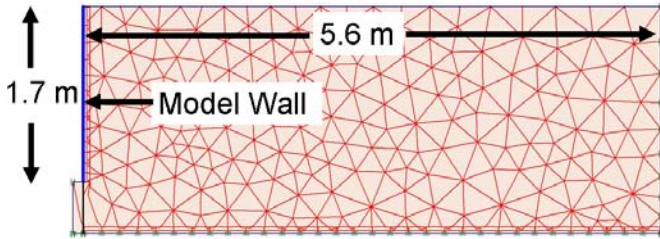


Fig. 10. FE model mesh for simulation of the soil container experiments

Stiff plate elements (1.7 meters tall) supported the soil laterally (Fig. 10), with the same weight as the experimental wall and supporting beam (Fig. 5). During simulation of the experiments, a friction interface ensured that the plate (wall) would move upwards with the adjacent soil elements as the lateral displacement was being applied.

## Soil Model

The employed Plaxis (2004) Hardening Soil (HS) model uses the Mohr-Coulomb failure rule, and a nonlinear hyperbolic stress-strain relationship (Fig. 11). All analyses were restricted to the pre-peak loading range, with numerically stable solutions.

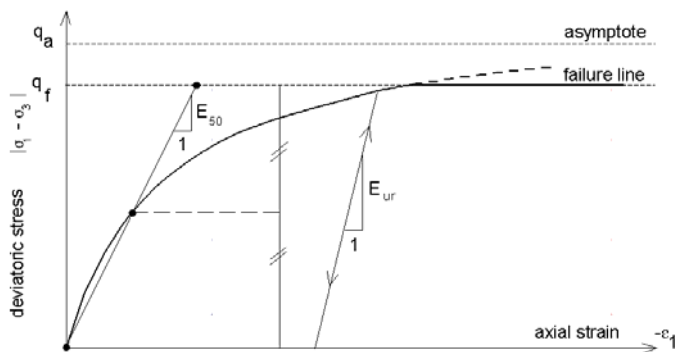


Fig. 11. Hyperbolic stress-strain relationship (Plaxis 2004)

For simulation of Test 2 (Soil T2, closest to the lab test condition), backfill shear strength parameters ( $\phi$  and  $c$ ) were determined based on the direct shear and triaxial tests (Table 1). The reference stiffness parameter  $E_{50}^{ref}$  (Fig. 11) was selected at a reference stress  $p_{ref} = 100$  kPa from the triaxial test stress-strain data according to a power law with  $m = 0.5$

(Plaxis 2004). Soil total unit weight was specified as  $\gamma = 20.6$  kN/m<sup>3</sup>, according to the field condition. A failure ratio ( $R_f = q_f/q_a$ , as shown in Fig. 11) value of  $R_f = 0.75$  was also adopted, which is within the range recommended by Duncan and Mokwa (2001). User manual recommendations and internal adjustments made by Plaxis (2004) determined the remaining HS model parameters.

For simulation of Test 1 (Soil T1, drier condition), backfill shear strength parameters (Table 1) were adjusted based on analysis of the observed passive failure wedge (Wilson 2009). A larger  $E_{50}^{ref}$  accounted for the experimentally observed higher stiffness compared with Test 2 (Fig. 9).

Table 1: FE model soil parameters

FE model parameter	Soil					Units
	T1 <sup>a</sup>	T2 <sup>a</sup>	D-S <sup>b</sup>	MD-SM <sup>b</sup>	MD-SC <sup>b</sup>	
$\phi$	52	46	38	33	23	degrees
$c$	13	14	0	24	95	kPa
$\psi$	22	16	8	3	0	degrees
$p^{ref}$	100	100	100	100	100	kPa
$m$	0.5	0.5	0.5	0.5	0.5	~
$E_{50}^{ref}$	50000	40000	35000	30000	30000	kN/m <sup>2</sup>
$E_{oed}^{ref}$	50000	40000	35000	30000	30000	kN/m <sup>2</sup>
$K_0^{nc}$	0.4	0.4	0.4	0.45	0.6	~
$g$	20.6	20.6	20	19	19	kN/m <sup>3</sup>
$R_f$	0.75	0.75	0.75	0.75	0.75	~

<sup>a</sup>Current experimental study

<sup>b</sup>Earth Mechanics Inc. (2005)

## Simulation Results

FE simulations of the soil container passive earth pressure experiments were made by prescribing a horizontal displacement boundary condition along the wall plate (left side of Fig. 10), while allowing free vertical displacement. Using this configuration, the wall moved upwards with the backfill in accordance with the experiments. As shown in Fig. 9, the FE models provide a satisfactory representation of the experimental load-displacement behavior.

## FE SIMULATIONS FOR A RANGE OF BACKFILL SOILS AND DEPTHS

In this section, FE Simulations are performed considering walls ranging from 1 meter (e.g., a pile cap, Rollins and Cole 2006) to 5 meters (e.g., a tall bridge abutment, Siddharthan et al. 1997) in height. Four different backfill soils are investigated to cover a range of likely backfill soil properties (Earth Mechanics 2005).

## Adjustments to the Model

In order to consider taller wall configurations, and to minimize potential interference with the model boundaries, these additional simulations were performed on extended and deepened backfill domains (Fig. 12), with dimensions determined through a trial and error process. Horizontal and vertical fixities were applied along the model base, with horizontal fixity also along the far end of the backfill and the soil domain beneath the model wall.

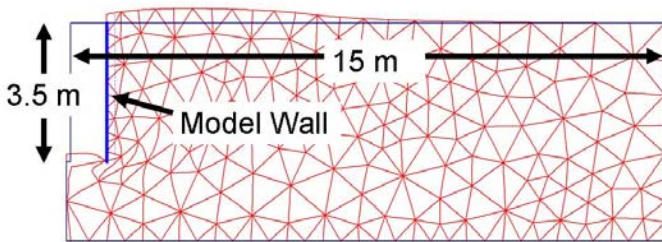


Fig. 12. Sample deformed mesh from simulation of a 3.5 meter tall wall with backfill Soil MD-SC

Lemnitzer et al. (2009), recently conducted a bridge abutment passive pressure experiment in which the test backwall displaced essentially solely in the horizontal direction. This was done in consideration of the potentially large friction force between the end of the bridge deck and the backwall (Lemnitzer et al. 2009), which may prevent vertical wall movement. In that configuration,  $\delta = 0.35\phi$  was measured at the instant of the peak measured load (Lemnitzer et al. 2009).

In the case of pile caps and integral abutments, a restriction from vertical wall uplift may also be anticipated (Duncan and Mokwa 2001). On that basis, a  $\delta = 0.35\phi$  interface  $R_{inter}$  (Plaxis 2004) was provided along the plate-soil boundary for the FE simulations. A horizontal displacement was again ascribed to the plate that represented the wall, but the vertical displacement was assigned as zero (Fig. 12), in accordance with the Lemnitzer et al. (2009) experiment.

Simulations were performed considering four soils (Soils T2, D-S, MD-SM, and MD-SC). Model parameters for these soils (Table 1) were determined based on conducted direct shear and triaxial tests (Earth Mechanics 2005) as described above for Soil T2. Soil T2 represents the placement condition backfill from Test 2 of the current experimental study. Soils D-S, MD-SM, and MD-SC represent three categories of sandy soils found in California in an extensive investigation of actual bridge abutment backfills (Earth Mechanics 2005). Soil D-S is dense (clean) sand, MD-SM is medium-dense silty sand, and MD-SC is medium-dense clayey sand.

## Simulation Results

Figs. 13 through 16 show the simulated passive force-displacement response, per meter of wall width, for the 4 soils mentioned above, considering wall heights  $H$  ranging from 1 to 3 meters. These curves are limited to the numerically stable

solution range, and may not fully reach the peak passive resistance. FE simulations of 4 and 5 meter walls were also conducted (shown further below in order to maintain a more reasonable scale in Figs. 13 through 16).

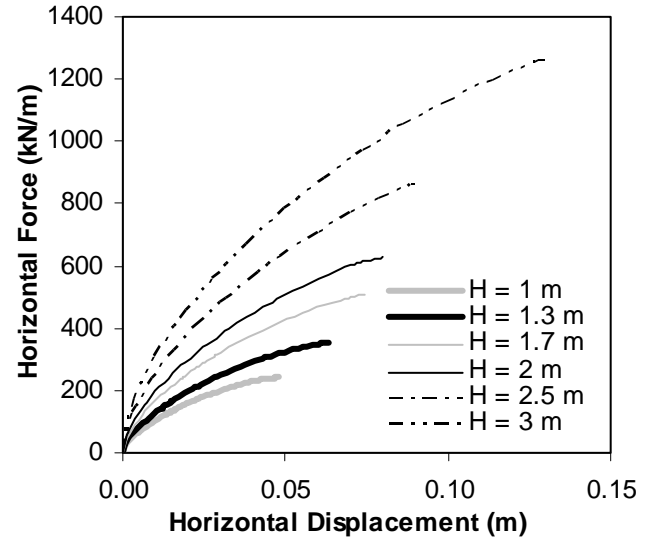


Fig. 13: Soil T2 ( $\phi = 46$  degrees,  $c = 14$  kPa,  $E_{50}^{ref} = 40,000$  kN/m<sup>2</sup>)

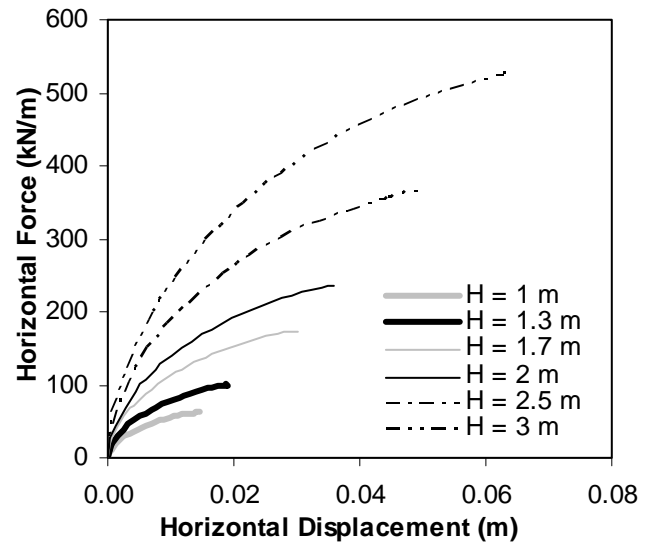


Fig. 14: Soil D-S ( $\phi = 38$  degrees,  $c = 0$  kPa,  $E_{50}^{ref} = 35,000$  kN/m<sup>2</sup>)

From Figs. 13 through 16, there is clearly a wide range in backfill strength and stiffness, depending on both the soil type and the wall height ( $H$ ). According to the FE model simulation with clean sand backfill (Soil D-S), the passive resistance with  $H = 3$  meters reached nearly 10 times that of the  $H = 1$  meter case (Fig. 14). The stiffness also increased rapidly as the wall became taller for Soil D-S (Fig. 14). For instance at a horizontal wall displacement of 1 centimeter, about 4.4 times the passive resistance was mobilized for  $H = 3$

meters, compared with  $H = 1$  meter (Fig. 14). In contrast, for the high  $c$  and lower  $\phi$  Soil MD-SC (Fig. 16), the passive resistance with  $H = 3$  meters reached only about 4 times that of the  $H = 1$  meter case, and the stiffness increase for taller walls was also less pronounced.

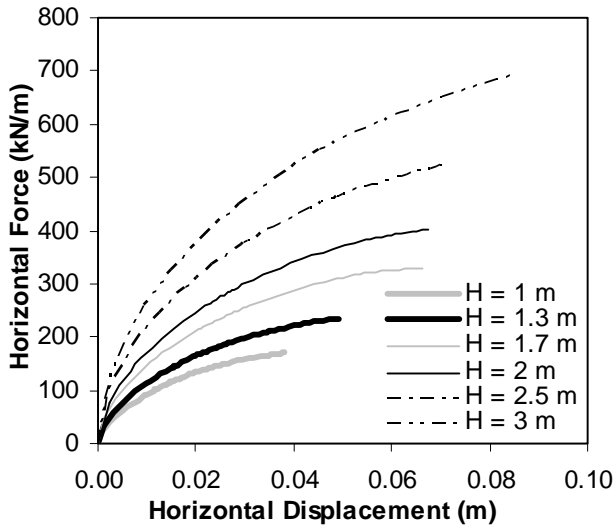


Fig. 15: Soil MD-SM ( $\phi = 33$  degrees,  $c = 24$  kPa,  $E_{50}^{ref} = 30,000$  kN/m<sup>2</sup>)

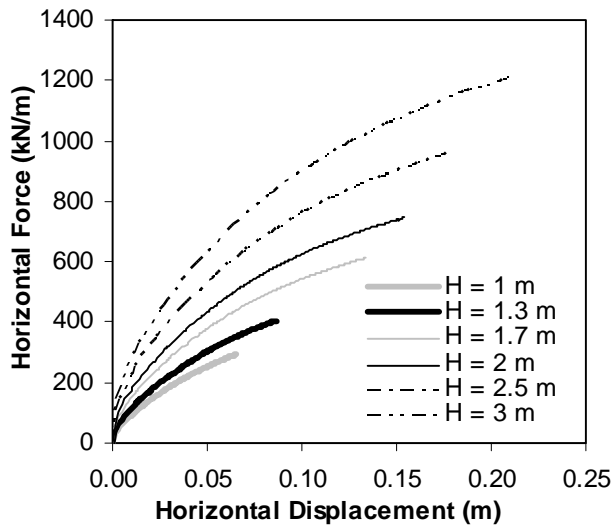


Fig. 16: Soil MD-SC ( $\phi = 23$  degrees,  $c = 95$  kPa,  $E_{50}^{ref} = 30,000$  kN/m<sup>2</sup>)

The drastic difference in load-displacement response for Soils T2 (Fig. 13) and D-S (Fig. 14) helps to further illustrate why it can be important to accurately account for the backfill soil strength and stiffness. Soil shear strength is often roughly approximated for earth pressure predictions, sometimes neglecting the cohesion in sandy soils (e.g., CSBC 2007). In some cases, it may be conservative (possibly resulting in costly over-design) to neglect cohesion and use a typical dense sand friction angle  $\phi = 38$  degrees (Earth Mechanics 2005), such as Soil D-S in Fig. 14. However when the passive pressure imposes loads which might damage the structure

(e.g., expansion of an integral abutment bridge), the opposite may be true. For instance, if a dense sand backfill similar to Soil T2 ( $\phi = 46$  degrees and  $c = 14$  kPa) were characterized with the more typical  $\phi = 38$  degrees, and  $c = 0$  values of Soil D-S, the passive resistance could be underestimated by a factor of more than 2 (Figs. 13 and 14).

Load-displacement simulations of the four backfill soils are also compared for the 1 and 5 meter tall wall in Figs. 17 and 18, respectively. Behind the 1 meter tall wall (Fig. 17), the highly cohesive Soil MD-SC was quite strong and preserved its stiffness over a large range of deflection. However, due to the higher confining stress conditions (Terzaghi et al. 1996) for the 5 meter wall (Fig. 18), the soil with the greatest  $\phi$  (T2) became the strongest and stiffest by a significant margin. Similarly, the cohesionless Soil D-S was clearly the weakest for the 1 meter wall (Fig. 17), but came close to matching Soils MD-SM and MD-SC in Fig. 18, due to its relatively high  $\phi$  and the deeper (5 meter) backfill.

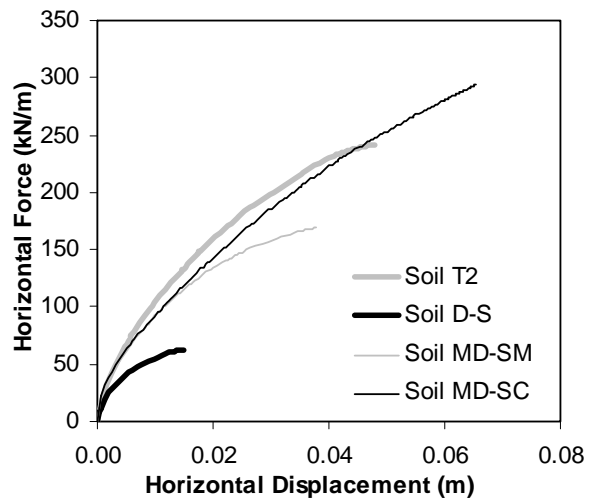


Fig. 17. Comparison of Soils T2, D-S, MD-SM, and MD-SC for a 1 meter tall wall

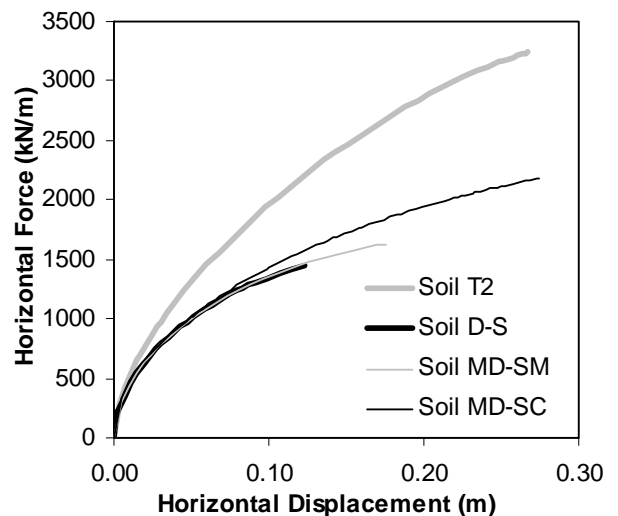


Fig. 18. Comparison of Soils T2, D-S, MD-SM, and MD-SC for a 5 meter tall wall

### Comparison of the Simulated Curves with Design Models

For use in bridge seismic design, AASHTO (2007) provides bi-linear abutment passive resistance models for “cohesive” and “non-cohesive” soils. Peak passive resistance ( $P_p$ ) and abutment stiffness ( $K_{abut}$ ) for the non-cohesive backfill model are derived from Equations (1) and (2):

$$P_p = p_p \times H_w \times w_w \quad (1)$$

$$K_{abut} = \frac{P_p}{F_w \times H_w} \quad (2)$$

where  $p_p$  is the passive lateral earth pressure,  $H_w$  is the wall height,  $w_w$  is the width, and  $F_w$  is a factor ranging from 0.01 for dense sands to 0.05 for compacted clays (Clough and Duncan 1991). For “non-cohesive,” non-plastic backfill (fines content < 30%), AASHTO (2007) provides an estimated  $p_p = 100H_w$  kPa. For cohesive backfill (clay fraction > 15%), AASHTO provides an estimated  $p_p = 240$  kPa.

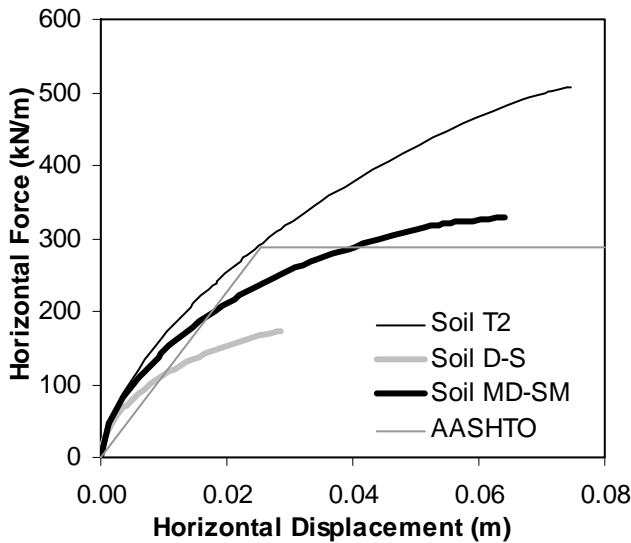


Fig. 19. Soils T2, D-S and MD-SM compared with the AASHTO (2007) bilinear model with  $F_w = 0.015$  for non-cohesive soil and a 1.7 meter tall wall

For a typical abutment sacrificial backwall height of 1.7 meters (Shamsabadi et al. 2007), Fig. 19 compares the FE curves with the AASHTO (2007) “non-cohesive” backfill model, for the soils that are closest to the criteria described above (T2, D-S, and MD-SM). A similar comparison is shown in Fig. 20 for a taller (3 meter) wall (Siddharthan et al. 1997). Figs. 21 (1.7 meter wall) and 22 (3 meter tall wall) compare the AASHTO (2007) “cohesive” backfill model, with the Soil MD-SC (which meets the above criteria) simulated force-displacement curve.

According to the simulation results for the 1.7 meter tall wall of Fig. 19, the AASHTO (2007) non-cohesive backfill model with  $F_w = 0.015$  provides a good match with Soil MD-SM, but significantly under and over predicts the resistance provided

by Soils T2, and D-S, respectively. For the 3 meter wall of Fig. 20, the AASHTO (2007) model provides a better representation for Soil T2, while over estimating in terms of both stiffness and capacity for Soils D-S and MD-SM.

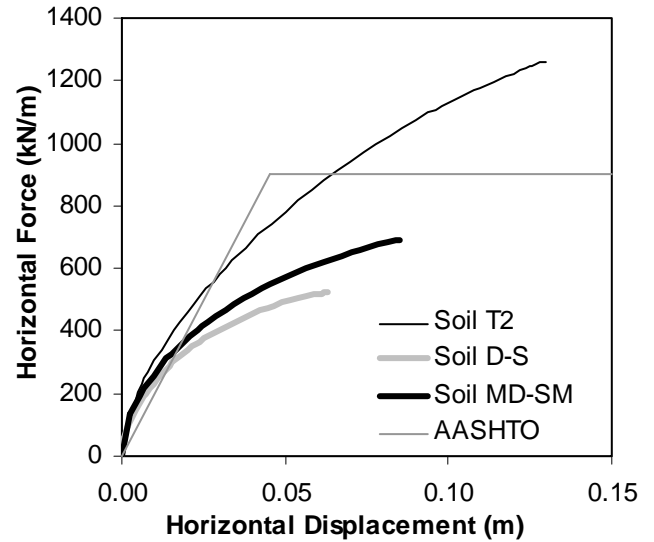


Fig. 20. Soils T2, D-S and MD-SM compared with the AASHTO (2007) bilinear model with  $F_w = 0.015$  for non-cohesive soil and a 3 meter tall wall

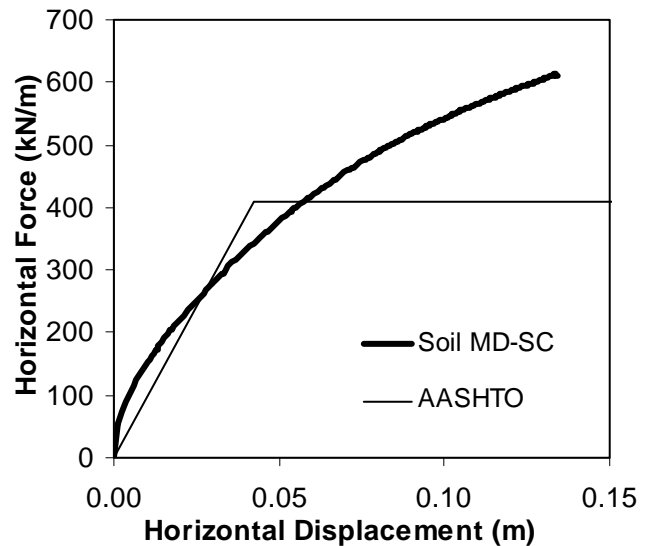


Fig. 21. Soil MD-SC compared with the AASHTO (2007) bilinear model with  $F_w = 0.025$  for cohesive soil and a 1.7 meter tall wall

For the 1.7 meter wall with Soil MD-SC, the AASHTO (2007) “cohesive” soil model with  $F_w = 0.025$  provides a satisfactory match in terms of stiffness, but underestimates the capacity (Fig. 21). With the 3 meter wall, the AASHTO (2007) model underestimates both the stiffness and capacity, compared with the FE model results (Fig. 22). Based on the comparisons in Figs. 19 through 22, higher order approximations of the



passive force-displacement relationship could clearly lead to a safer or more economic design.

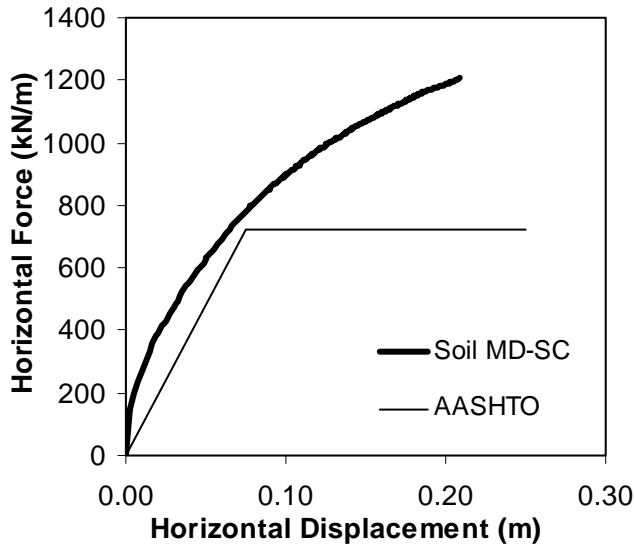


Fig. 22. Soil MD-SC compared with the AASHTO (2007) bilinear model with  $F_w = 0.025$  for cohesive soil and a 3 meter tall wall

#### HYPERBOLIC LOAD-DISPLACEMENT MODELS

Hyperbolic models have been shown to provide a good representation of the passive load-deflection behavior up to the peak resistance (Duncan and Mokwa 2001, Cole and Rollins 2006, Shamsabadi et al. 2007). Duncan and Mokwa (2001) employed a model defined by the initial stiffness ( $K_{max}$ ) according to the following equation:

$$F(y) = \frac{y}{\frac{1}{K_{max}} + R_f \frac{y}{F_{ult}}} \quad (3)$$

where  $F$  is the resisting force,  $y$  is the horizontal displacement,  $F_{ult}$  is the maximum passive resistance, and  $R_f$  is a failure ratio.

Such hyperbolic models can be used as nonlinear springs to represent the passive earth pressure load-displacement resistance. For dynamic simulations, a material (“hyperbolicgapmaterial”) is also available for use as a spring in the finite element code OpenSees (Mazzoni et al. 2006). The “hyperbolicgapmaterial” implements a backbone curve using hyperbolic model Equation (3), an adjustable expansion gap, and a linear unloading and reloading stiffness approximation (Wilson and Elgamal 2008, Dryden 2009, Wilson 2009).

Hyperbolic model parameters are provided in Tables 2 through 5 as approximations of the FE simulation results (Figs. 23 through 26). These models can be scaled according to the structure width, with an applied 3D correction factor in the case of narrow walls (e.g. Brinch-Hansen 1966). Using  $F_{ult}$  based on the Log Spiral prediction, the additional

parameters were selected to match the FE curves. Compared with the bi-linear models shown in Figs. 19-22, the hyperbolic curves clearly provide a superior representation of the passive force-displacement relationship.

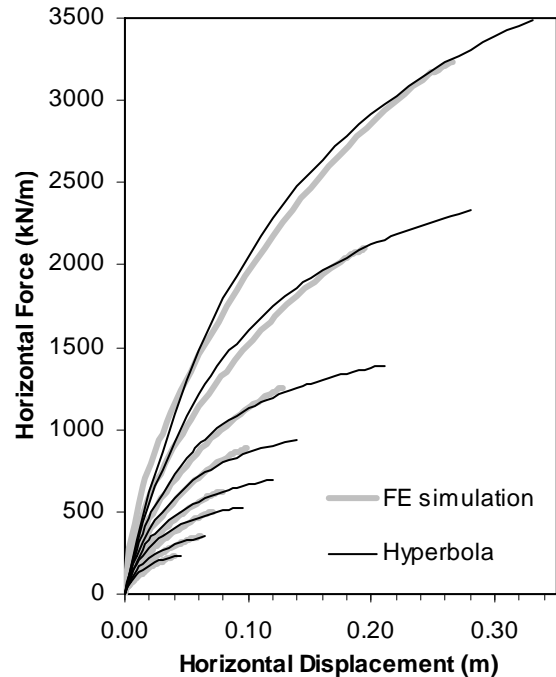


Fig. 23: FE simulated force-displacement curves for Soil T2 (1, 1.3, 1.7, 2, 2.5, 3, 4 and 5 meter tall walls) and hyperbolic model approximations

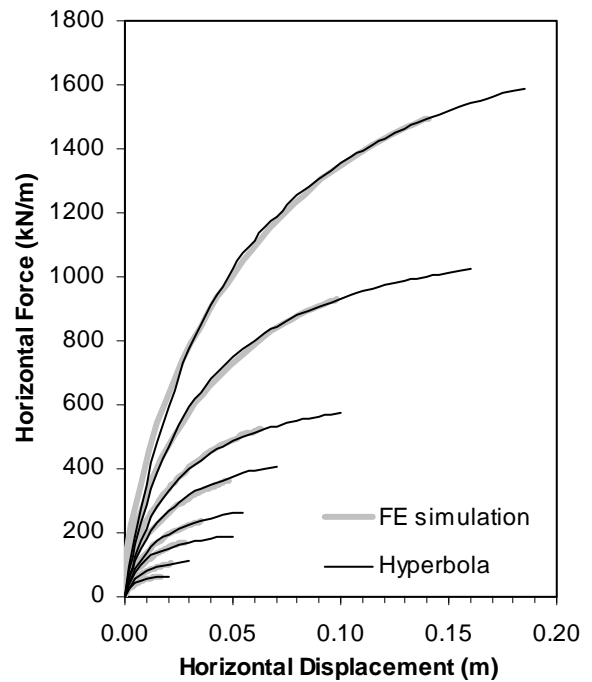


Fig. 24: FE simulated force-displacement curves for Soil D-S (1, 1.3, 1.7, 2, 2.5, 3, 4 and 5 meter tall walls) and hyperbolic model approximations

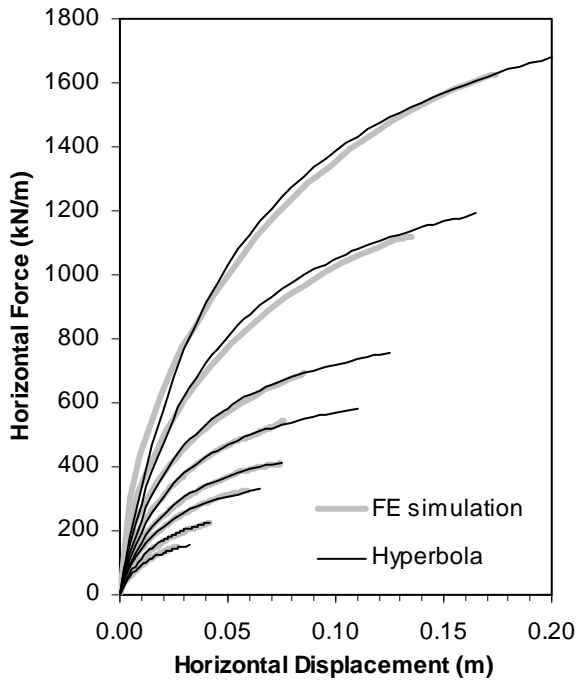


Fig. 25: FE simulated force-displacement curves for Soil MD-SM (1, 1.3, 1.7, 2, 2.5, 3, 4 and 5 meter tall walls) and hyperbolic model approximations

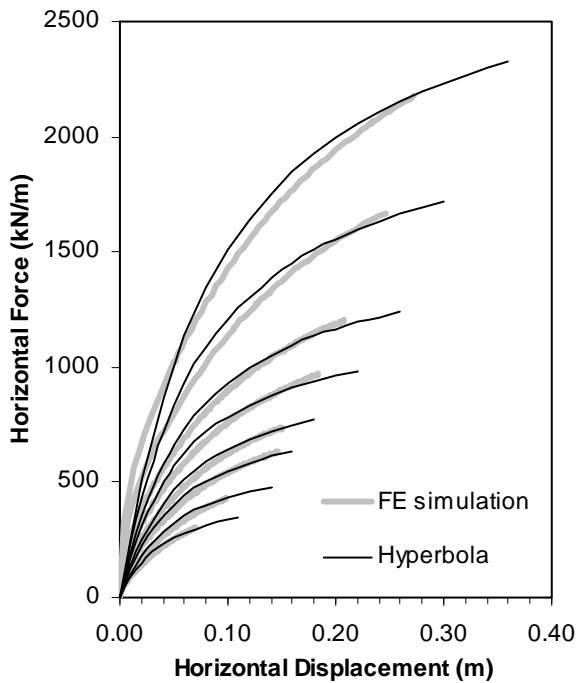


Fig. 26: FE simulated force-displacement curves for Soil MD-SC (1, 1.3, 1.7, 2, 2.5, 3, 4 and 5 meter tall walls) and hyperbolic model approximations

Table 2. Hyperbolic model parameters for Soil T2

Soil T2			
H (m)	$K_{max}$ (kN/cm/m)	$R_f$	$F_{ult}$ (kN/m)
1	180	0.7	230
1.3	210	0.75	350
1.7	240	0.8	550
2	250	0.8	725
2.5	280	0.85	1050
3	310	0.85	1450
4	330	0.8	2350
5	350	0.75	3500

Table 3. Hyperbolic model parameters for Soil D-S

Soil D-S			
H (m)	$K_{max}$ (kN/cm/m)	$R_f$	$F_{ult}$ (kN/m)
1	170	0.8	65
1.3	200	0.8	110
1.7	240	0.8	190
2	250	0.8	265
2.5	280	0.8	410
3	310	0.85	600
4	380	0.85	1000
5	420	0.8	1600

Table 4. Hyperbolic model parameters for Soil MD-SM

Soil MD-SM			
H (m)	$K_{max}$ (kN/cm/m)	$R_f$	$F_{ult}$ (kN/m)
1	160	0.7	155
1.3	180	0.7	225
1.7	210	0.75	325
2	230	0.75	410
2.5	270	0.8	575
3	310	0.8	750
4	350	0.8	1200
5	400	0.8	1700

Table 5. Hyperbolic model parameters for Soil MD-SC

Soil MD-SC			
H (m)	$K_{max}$ (kN/cm/m)	$R_f$	$F_{ult}$ (kN/m)
1	110	0.75	365
1.3	130	0.75	485
1.7	150	0.75	650
2	180	0.8	775
2.5	210	0.8	1000
3	230	0.8	1250
4	270	0.8	1750
5	320	0.8	2350

## CONCLUSIONS

Large scale passive earth pressure load-displacement tests were presented, along with FE simulations. In the conducted low  $\delta_{mob}$  (2 to 3 degrees) experiments: i) the measured peak passive pressure was close to the Coulomb and Log Spiral predictions, and ii) using shear strength parameters determined from laboratory tests and analysis of the experiments, FE model simulations provided a satisfactory representation of the load-displacement behavior up to the peak resistance.

A series of passive pressure numerical simulations was performed next, considering four different backfills and a range of wall heights. Results show how the different backfill soils can provide substantially different load-displacement resistance, in terms of both stiffness and strength. It was also shown that the increase in supported backfill height, and the depth dependent stiffness of the soil, contributes to significant variations in the available resistance.

For practical applications, hyperbolic model approximations were provided for 32 different combinations of backfill soil type and wall height. Such hyperbolic models can be used as nonlinear springs to represent the passive earth pressure load-displacement resistance in pushover analyses and dynamic simulations.

## ACKNOWLEDGEMENTS

Support for this research was provided by the National Science Foundation (NSF) NEES-R grant number 0420347 under the overall direction of Professor M. Saiid Saiidi of the University of Nevada at Reno (UNR). Professor Scott Ashford kindly allowed for use of the large soil container. Financial support for the 1st author in the form of the UCSD Robert and Natalie Englekirk Fellowship is also gratefully acknowledged. Dr. Chris Latham, Dr. Anoosh Shamsabadi, and Dr. Azadeh Bozorgzadeh provided much help and insight during the planning stages. The success of the experimental phase would not have been possible without the help of Alex Sherman, Lonnie Rodriguez, Mike Dyson and the entire Englekirk Structural Engineering Center staff. Dr. Arul Arulmoli of Earth Mechanics, Inc., Joe Vettel of Geocoin Inc., and James Ward and Allan Santos of Leighton and Associates are all gratefully acknowledged for services donated regarding backfill material testing.

## REFERENCES

AASHTO [2007]. *Proposed Guide Specifications for LRFD Seismic Bridge Design*. American Association of State Highway and Transportation Officials, Washington D.C.

Bozorgzadeh, A. [2007]. "Effect of structure backfill on stiffness and capacity of bridge abutments." Ph.D. Thesis, Dept. of Structural Eng., University of California, San Diego, CA.

Brinch-Hansen, J. [1966]. "Resistance of a Rectangular Anchor Slab." *Bulletin No. 21.*, Danish Geotechnical Institute, Copenhagen, 12-13.

Caltrans [2004]. "Seismic design criteria, version 1.3." California Dept. of Transportation, Sacramento, CA.

Caltrans [2006]. "Standard specifications." California Dept. of Transportation, Sacramento, CA.

Clough, G. W., and Duncan, J. M. [1991]. *Foundation engineering handbook*, 2nd Ed., H. Y. Fang, ed., Chapman and Hall, New York, NY.

Cole, R., and Rollins, K. [2006]. "Passive earth pressure mobilization during cyclic loading." *Journal of Geotechnical and Geoenvironmental Engineering*, 132(9), 1154-1164.

CBSC [2007]. "California building code." California Building Standards Commission. Sacramento, CA.

Duncan, M., and Mokwa, R. [2001]. "Passive earth pressures: theories and tests." *Journal of Geotechnical and Geoenvironmental Engineering*, 127(3), 248-257.

Dryden, G. M. [2009]. "The integration of experimental and simulation data in the study of reinforced concrete bridge systems including soil-foundation-structure-interaction." Ph.D. Thesis, Dept. of Civil and Environmental Eng., University of California, Berkeley, CA.

Earth Mechanics, Inc. [2005]. *Field investigation report for abutment backfill characterization*. UCSD Report No. SSRP-05/02, Department of Structural Engineering, University of California, San Diego, La Jolla, CA.

Fang, Y., Chen, T., Holtz, R. and Lee, W. [2004]. "Reduction of boundary friction in model tests." *Geotechnical Testing Journal*, 27(1), 3-12.

Gadre, A., and Dobry, R. [1998]. "Lateral cyclic loading centrifuge tests on square embedded footing." *Journal of Geotechnical and Geoenvironmental Engineering*. 124(11), 1128-1138.

Lemnitzer, A., Ahlberg, E., Nigbor, R., Shamsabadi, A., Wallace, J., and Stewart, J. [2009]. "Lateral performance of full-scale bridge abutment backwall with granular backfill," *Journal of Geotechnical and Geoenvironmental Engineering*, April, 506-514.

Mazzoni, S., McKenna, F., and Fenves, G. [2006]. *Open System for Earthquake Engineering Simulation User Manual*. Pacific Earthquake Engineering Research Center, University of California, Berkeley, CA, USA.

McCarthy, D. [2007]. *Essentials of Soil Mechanics and Foundations*, 7th Ed., Prentice Hall, Upper Saddle River, New Jersey.

Peric, D., Shah, B. and Esmaily, A. [2007]. “Three dimensional finite element modeling of integral bridges subjected to thermal loading.” *Proceedings, ANNIE 2007*, St. Louis, Missouri.

Plaxis [2004]. Plaxis V8, Brinkgreve, R., and Broere, W. ed. PLAXIS, AN DELFT, Netherlands.

Rollins, K. and Cole, R. [2006]. “Cyclic lateral load behavior of a pile cap and backfill.” *Journal of Geotechnical and Geoenvironmental Engineering*, 132(9), 1143-1153.

Shah, B. [2007]. “3D finite element analysis of integral abutment bridges subjected to thermal loading,” Masters thesis, Dept. of Civil Engineering, Kansas State University.

Shamsabadi, A., Rollins, K., and Kapuskar, M. [2007]. “Nonlinear soil-abutment-bridge structure interaction for seismic performance-based design.” *Journal of Geotechnical and Geoenvironmental Engineering*, 133(6), 707-720.

Siddharthan, R. El-Gamal, M. and Maragakis, E. [1997]. “Stiffness of abutments on spread footings with cohesionless backfill.” *Canadian Geotechnical Journal* 34, 686-697.

Terzaghi, K., Peck, R., and Mesri, G. [1996]. *Soil mechanics in engineering practice*, 3rd edition, John Wiley and Sons, Inc. New York, NY.

Wilson, P. and Elgamal, A. [2008]. “Full scale bridge abutment passive earth pressure tests and calibrated models,” *Proceedings, The 14th World Conference on Earthquake Engineering*, Beijing, China.

Wilson, P. and Elgamal, A. [2009]. “Full-scale shake table investigation of bridge abutment lateral earth pressure,” *Bulletin of the New Zealand Society for Earthquake Engineering*, NZSEE 42(1).

Wilson, P. [2009]. “Large Scale Passive Force-Displacement and Dynamic Earth Pressure Experiments and Simulations.” Ph.D. thesis, Dept. of Structural Eng., University of California, San Diego, CA.